Meteoritics & Planetary Science 37, 329–344 (2002)
Available online at http://www.uark.edu/meteor

Impact processing of chondritic planetesimals: Siderophile and volatile element fractionation in the Chico L chondrite

MARC D. NORMAN[1,3]* AND DAVID W. MITTLEFEHLDT[2]

[1]Lunar and Planetary Institute, 3600 Bay Area Boulevard, Houston, Texas 77058, USA
[2]Mail Code SR, NASA Johnson Space Center, Houston, Texas 77058, USA
[3]Research School of Earth Sciences, Australian National University, Canberra ACT 0200, Australia
*Correspondence author's e-mail address: marc.norman@anu.edu.au

(Received 2001 February 2; accepted in revised form 2001 November 21)

Abstract–A large impact event 500 Ma ago shocked and melted portions of the L-chondrite parent body. Chico is an impact melt breccia produced by this event. Sawn surfaces of this 105 kg meteorite reveal a dike of fine-grained, clast-poor impact melt cutting shocked host chondrite. Coarse (1–2 cm diameter) globules of FeNi metal + sulfide are concentrated along the axis of the dike from metal-poor regions toward the margins. Refractory lithophile element abundance patterns in the melt rock are parallel to average L chondrites, demonstrating near-total fusion of the L-chondrite target by the impact and negligible crystal-liquid fractionation during emplacement and cooling of the dike.

Significant geochemical effects of the impact melting event include fractionation of siderophile and chalcophile elements with increasing metal-silicate heterogeneity, and mobilization of moderately to highly volatile elements. Siderophile and chalcophile elements ratios such as Ni/Co, Cu/Ga, and Ir/Au vary systematically with decreasing metal content of the melt. Surprisingly small (~10^2) effective metal/silicate-melt distribution coefficients for highly siderophile elements probably reflect inefficient segregation of metal despite the large degrees of melting. Moderately volatile lithophile elements such K and Rb were mobilized and heterogeneously distributed in the L-chondrite impact breccias whereas highly volatile elements such as Cs and Pb were profoundly depleted in the region of the parent body sampled by Chico. Volatile element variations in Chico and other L chondrites are more consistent with a mechanism related to impact heating rather than condensation from a solar nebula. Impact processing can significantly alter the primary distributions of siderophile and volatile elements in chondritic planetesimals.

INTRODUCTION

About 500 Ma ago a massive, possibly catastrophic collision rocked the L-chondrite parent body (Nakamura *et al.*, 1990; Bogard *et al.*, 1995; Haack *et al.*, 1996). Petrographic evidence for one or more large impact events includes shock-induced partial melting and high-pressure phases such as majorite and diamond in several L chondrites, indicating shock stage S6 and transient pressures of 75–90 GPa (see review by Brearley and Jones, 1998). Highly volatile trace elements typically are depleted in heavily shocked L chondrites compared to unshocked or mildly shocked L chondrites (Keays *et al.*, 1971; Huston and Lipschutz, 1984; Walsh and Lipschutz, 1982). Argon isotopic compositions of L chondrites are often disturbed or reset, with K-Ar and U-Th-He gas retention ages providing clear evidence for significant heating at ~500 Ma that is most plausibly attributed to a collision of the L-chondrite parent body with another asteroid at that time (Bogard *et al.*, 1995; Wasson and Wang, 1991 and references therein).

Impact melt breccias with bulk elemental and oxygen isotopic compositions similar to L chondrites offer direct evidence for energetic collisions. Examples include Patuxent Range (PAT) 91501 (Mittlefehldt and Lindstrom, 2001; Harvey and Roedder, 1994), Shaw (Taylor *et al.*, 1979), Point of Rocks (Nakamura *et al.*, 1990), Ramsdorf (Yamaguchi *et al.*, 1999), and Chico (Bogard *et al.*, 1995), all of which contain variable amounts of clast-poor impact melt breccia with igneous textures and immiscible segregations of metal and sulfide. Rubidium-strontium internal isochron ages of 460 ± 11 Ma (Nakamura *et al.*, 1990) and 467 ± 15 Ma (Fujiwara and Nakamura, 1992) on melt breccia from Point of Rocks and Chico, respectively, fix the age of impact melting in these meteorites. ^{40}Ar-^{39}Ar ages of the Chico impact melt are somewhat older and more variable, with a minimum age of ~530 Ma (Bogard *et al.*, 1995). The older ^{40}Ar-^{39}Ar ages probably reflect incomplete outgassing, even in samples that were completely melted (Bogard *et al.*, 1995). The Shaw L chondrite has ^{40}Ar-^{39}Ar age of ~4.3 Ga (Bogard and Hirsch, 1980) and a U-Th-He gas

Prelude preprint MS#4505
© Meteoritical Society, 2002. Printed in USA.

retention age of ~3.5 Ga (Wasson and Wang, 1991) indicating this impact melt breccia formed in a much earlier event.

The gas retention ages and cosmic-ray exposure ages are consistent with most L chondrites being derived from one immediate parent object, although a cosmic-ray age spike at ~40 Ma could indicate that some L chondrites were derived from a separate object (Marti and Graf, 1992; Wasson and Wang, 1991). Nevertheless, multiple immediate parent objects could still have been derived from a single, original L-chondrite parent body, and we will assume this to be the case. Thermal models are consistent with disruption and cooling of the L-chondrite parent body as a self-insulating rubble pile with an effective thickness on the order of ~1 km (Haack *et al.*, 1996).

To investigate the petrological and geochemical consequences of a large impact event on a chondritic planetesimal, we studied the major and trace element composition of Chico, a 105 kg L chondrite composed of a dike of clast-poor impact melt cutting heavily shocked chondritic wallrock. Previously recognized features of Chico that motivated this study include the igneous texture and centimeter-size globules of metal and sulfide in the impact melt, variable K/Ca ratios, and depletion of highly volatile elements such as Cd and Tl in both the impact melt and the host chondrite (Nakamura *et al.*, 1990; Bogard *et al.*, 1995; Yolcubal *et al.*, 1997). Chico provides a natural laboratory in which to study siderophile and volatile element fractionation during collisional processing of chondritic planetesimals.

PETROGRAPHY AND GEOLOGY OF L-CHONDRITE IMPACT MELTS

La Paz (1954) provided a macroscopic description of Chico and the circumstances of its discovery, noting the irregular distribution of metal, a correlation of metal abundance and texture, and the presence of an extraordinarily large (5.7 × 4.4 cm) "chondrus" that turned out to be a rounded clast of the chondrite country rock surrounded by impact melt (Bogard *et al.*, 1995). Rubin (1985) listed Chico as a chondritic impact breccia, and Scott *et al.* (1986) suggested that the Chico and Point of Rocks meteorites are probably paired based on similar impact melt textures. Macroscopic and petrologic descriptions of Chico, including mineral and glass compositions, are given by Scott *et al.* (1986), Bogard *et al.* (1995), and Garrison *et al.* (1992).

Sawn faces of Chico reveal a 30 cm wide zone of clast-poor impact melt cutting shocked and brecciated host chondrite. The impact melt zone is interpreted as an intrusive dike based on the following evidence: (1) chondrules in the host chondrite are fractured, sheared, and truncated in sharp contact against the melt rock; (2) margins of the melt zone are quenched against the host chondrite; (3) olivine and pyroxene grain size increases toward the center of the melt zone; (4) clast content decreases toward the center of the melt zone; (5) metallic globules are concentrated along the center of the melt zone suggestive of flow differentiation; and (6) size of metallic globules increases toward the center of the melt zone (Bogard *et al.*, 1995). These features are consistent with injection of the impact melt into the wall or basement floor of a crater rather than as ejecta on the surface of the parent body or an *in situ* partial melt (Stöffler *et al.*, 1991; also see discussion of PAT 91501 in Mittlefehldt and Lindstrom, 2001).

Igneous textures of the silicate melt and metallic globules demonstrate near-total melting of the L-chondrite target by the impact event. The impact melt in Chico crystallized into fine-grained, randomly oriented, euhedral olivines and pyroxenes in a matrix of interstitial albitic glass (Fig. 1). Olivines in the center of the melt zone are <100 μm wide and pyroxenes are 1–2 mm long. Metallic globules in the impact melt range in size up to 2 cm in diameter. These globules are composed of FeNi metal, troilite, and schreibersite, and they have weakly developed dendritic textures indicating crystallization of a melt. Many of these metallic globules show coronae of metal or sulfide in the interstices of the adjacent silicate melt (Fig. 1), which could represent either quenching of the melt during the final stages of metal migration and globule growth, or backflow of liquid metal or sulfide into the silicate during quenching (E. R. D. Scott and G. J. Taylor, pers. comm., 1998). The host chondrite is shocked to stage S6 of Stöffler *et al.* (1991). It contains pockets of silicate melt, veins of shock-mobilized metal, and fractured chondrules.

Chico is one of several L-chondrite breccias produced by large degrees of impact melting. The petrography and age of Point of Rocks is very similar to Chico (Nakamura *et al.*, 1990; Scott *et al.*, 1986; Bogard *et al.*, 1995). PAT 91501 has an igneous texture with a grain size coarser than Chico: olivines in PAT 91501 are 100–500 μm up to a maximum of 1.7 mm and pyroxenes are up to ~2.7 mm long (Mittlefehldt and Lindstrom, 2001). Plagioclase is present in PAT 91501 but absent in the Chico melt breccia where the plagioclase component is contained in the matrix glass. The L-chondrite Shaw consists of a centimeter-scale mixture of impact melt and chondritic country rock (Taylor *et al.*, 1979). The melt lithology in Shaw has a grain size similar to PAT 91501. Metal in Shaw is heterogeneously distributed on the centimeter scale although a point count of a large slab shows that the bulk meteorite is not depleted in metal relative to average L chondrites (Taylor *et al.*, 1979). Ramsdorf consists of a more intimate mixture of clast-poor impact melt and partially melted chondritic lithologies that differs from the well-defined cross-cutting relations seen in Chico (Yamaguchi *et al.*, 1999). The ghost chondrules observed in Ramsdorf suggests that this meteorite may represent chondritic country rock that was internally melted by shock heating rather than being intruded by impact melt (Yamaguchi *et al.*, 1999).

Chico, PAT 91501, Shaw, and Ramsdorf appear to represent a continuum of lithologies related to impact melting on the L-chondrite parent body. Chico may represent either a smaller volume of melt or a more distal region of a dike that cooled more rapidly, whereas PAT 91501 represents either a larger volume of melt or a more proximal region of a dike that cooled

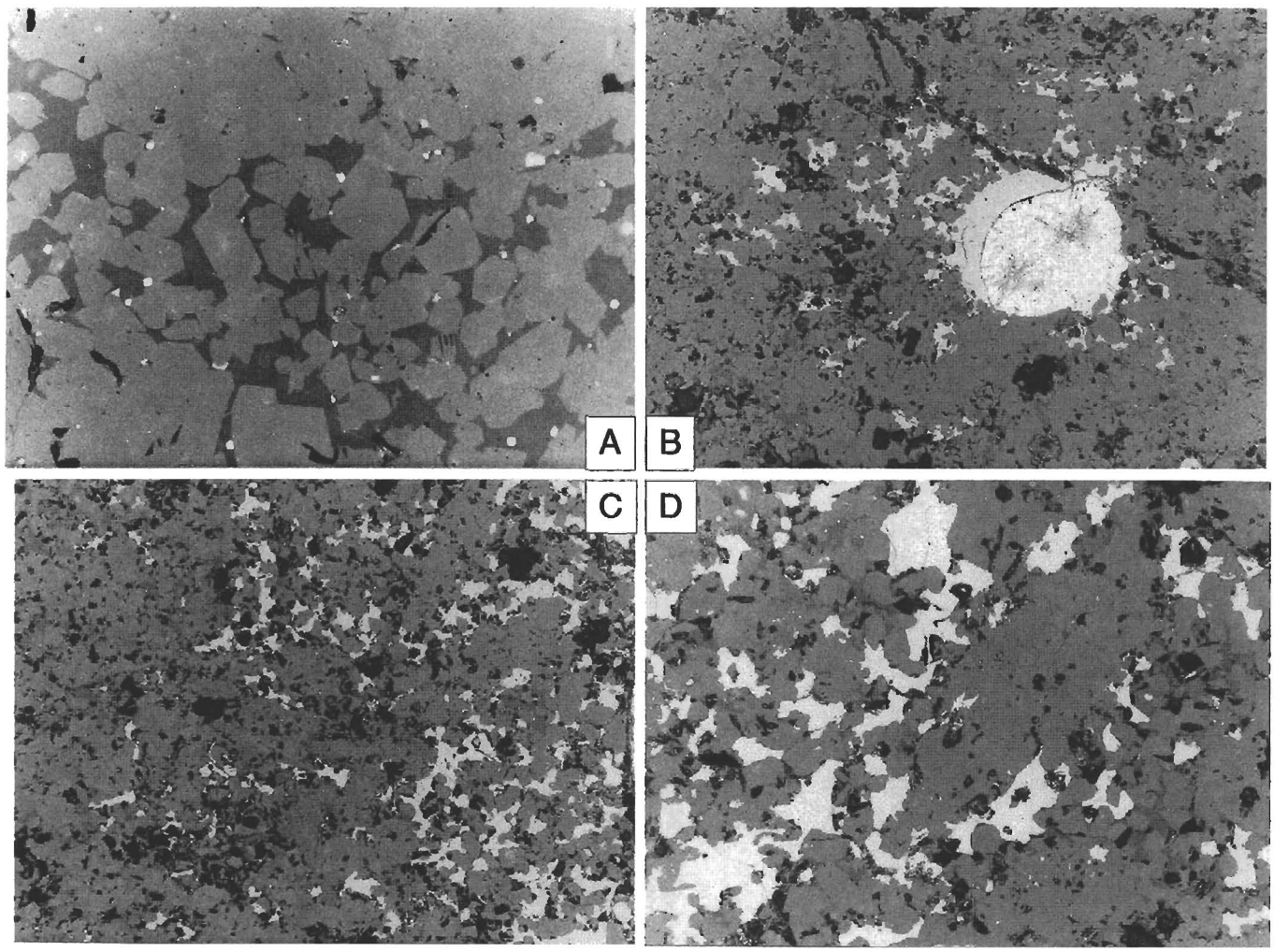

FIG. 1. Reflected light photomicrographs of the Chico impact melt. (a) Impact melt breccia composed of euhedral olivine, pyroxene, and interstitial glass. Small blebs of highly reflective metal are adhering to the surfaces of silicate grains. Field of view is 0.25 mm. (b) A metallic bleb composed of FeNi and FeS surrounded by a corona of metal and sulfide grading outward to regions of melt relatively depleted in metal. Field of view is 1 mm. (c) Impact melt adjacent to a large metallic globule demonstrating the gradation in abundance of interstitial metal away from the globule. Field of view is 1 mm. (d) View showing the distribution of metal and sulfide interstitial to olivine and pyroxene. Field of view is 0.5 mm.

more slowly. Ramsdorf may represent country rock that was internally heated and melted *in situ*. The contrasting ages of Chico and Shaw imply that the L-chondrite parent body suffered at least two collisions that were sufficiently energetic to produce clast-poor impact melt, and that multiple generations of melt are present. Predictions of this model would be that grain size is variable and metal is distributed heterogeneously on the L-chondrite parent body, with regions of coarse-grained, metal-poor silicate melt breccia and other (deeper?) areas enriched in metal. The scale of this heterogeneity must be at least the size of PAT 91501 (20 cm).

ANALYTICAL PROCEDURES

Major and trace element compositions of impact melt and host chondrite from Chico were determined by instrumental neutron activation analysis (INAA) and inductively-coupled plasma mass spectrometry (ICPMS) with samples taken from the same cores previously used for Ar isotopic studies (Bogard *et al.*, 1995). Handpicked rock chips (20–80 mg) were analyzed by INAA following procedures described by Mittlefehldt and Lindstrom (1993). One sample of the Point of Rocks impact melt, and a metal globule from the Chico impact melt were also analyzed by INAA (Table 1). Prior to analysis the metal particle was cleaned in an ultrasonic bath using distilled ethanol and high-purity water. For the ICPMS analyses (Table 2), ~1 g splits of the cores were crushed to a coarse powder using a steel piston mortar, and ~100 mg splits were dissolved in duplicate using distilled HF-HNO_3. The solution was brought to final volume in 2% HNO_3 and analyzed with a quadrupole ICPMS following procedures described by Norman *et al.* (1998).

TABLE 1. INAA analyses of the Chico and Point of Rocks L chondrites.*

	Melt rock										Host chondrite						Metal
	1-1	1-2	2-1	2-2	4	7	8-1	8-2	87.9a	Pt o'Rx	3-1	3-2	4	6-1	6-2	87.5b	8M
Wt (mg)	47.63	45.82	47.6	59.77	55.44	39.87	49.07	39.19	53.07	77.8	51.74	64.47	61.09	58.66	63.4	19.71	38.30
Na_2O (%)	0.88	0.90	1.13	1.13	1.14	1.12	0.92	0.74	0.95	0.73	0.89	0.88	0.84	0.94	0.94	0.95	–
K_2O (%)	0.20	0.25	0.10	0.12	0.22	<0.13	0.14	<0.14	0.22	0.15	0.10	0.10	0.15	0.12	0.10	0.09	–
CaO (%)	1.4	1.7	1.8	2.1	1.9	1.7	1.6	1.4	1.8	1.7	1.5	2.0	1.8	1.7	1.6	1.4	–
FeO (%)	22.7	23.1	18.4	18.3	17.9	18.4	20.3	24.5	20.4	22.3	27.5	27.0	27.5	27.8	29.2	27.3	–
Sc	9.0	9.0	9.8	9.9	10.1	9.8	9.2	8.2	9.3	8.7	8.7	8.8	8.7	8.7	9.2	6.5	–
Cr	4190	4200	4420	4470	4440	4550	4260	4030	4290	4150	4180	3670	3660	3450	3320	4590	81
Co	355	375	111	104	89	114	170	449	245	312	572	532	688	620	713	554	6680
Ni	7430	7660	1920	1770	1280	2050	2950	8920	4810	5940	12500	12400	11700	12800	16600	12120	131000
La	0.32	0.32	0.37	0.37	0.38	0.38	0.35	0.29	0.35	0.31	0.32	0.25	0.33	0.33	0.30	0.47	–
Sm	0.209	0.208	0.233	0.247	0.251	0.242	0.223	0.188	0.236	0.204	0.216	0.182	0.202	0.219	0.204	0.272	–
Eu	0.074	0.083	0.093	0.089	0.081	0.092	0.081	0.083	0.089	0.084	0.087	0.081	0.079	0.081	0.091	0.093	–
Tb	0.043	0.049	0.059	0.062	0.043	0.056	0.057	0.070	0.057	0.055	<0.10	<0.09	<0.12	<0.12	0.050	0.056	–
Yb	0.252	0.250	0.270	0.274	0.295	0.296	0.263	0.202	0.277	0.248	0.230	0.220	0.270	0.240	0.220	0.240	–
Lu	0.042	0.041	0.040	0.046	0.046	0.047	0.042	0.039	0.039	0.032	0.031	0.038	0.039	0.031	0.037	0.040	–
Hf	0.15	0.20	0.22	0.22	0.19	0.14	0.17	0.17	0.19	0.19	–	–	0.23	0.29	0.21	–	–
As	0.81	0.97	0.31	0.22	0.27	0.34	0.33	1.25	0.53	0.74	1.52	1.74	1.68	3.42	2.17	1.89	18.1
Se	6.6	6.6	2.8	2.7	1.9	2.7	4.2	8.5	4.1	8.9	10.1	10.0	6.3	8.1	10.0	10.3	–
Sb	0.33	<0.09	<0.03	<0.03	<0.05	<0.05	<0.03	0.05	<0.04	0.04	0.09	0.11	0.04	0.36	0.06	0.06	0.43
Ir (ppb)	248	239	45.2	37.8	51.5	46.5	52.9	321	194	92	496	507	580	522	690	430	10400
Au (ppb)	92.9	89.2	24.7	22.5	16.8	26	41.3	125	62.4	74.3	177	174	178	175	230	181	1994

*Data in ppm except as noted.

TABLE 2. ICPMS analyses of the Chico L chondrite.*

Sample	1A	1B	2A	2B	3A	3B	4A	4B	6A	6B	7A	7B	8A	8B	9A	9B
Wt (mg)	102.7	104.6	102.5	103.2	102.9	103.0	104.8	106.3	105.4	106.2	102.5	103.0	107.2	104.0	104.5	104.3
Lithology	Melt		Melt		Chondrite		Melt		Chondrite		Melt		Melt		Melt	
Li	2.2	2.2	2.4	2.3	2.0	1.9	1.9	2.0	1.9	1.8	2.1	2.1	2.1	2.1	2.4	2.4
Sc	9.2	9.1	10.7	10.4	9.1	8.2	9.8	9.5	8.1	8.5	9.9	10.5	10.4	10.0	9.5	9.3
Ti	677	661	771	745	625	587	705	696	577	604	696	734	727	710	682	675
V	77	76	86	85	72	71	79	79	67	70	80	84	85	81	77	77
Cr	3698	3673	4177	4132	3424	3581	3906	3988	3343	3501	4021	4241	4276	4105	3898	3867
Mn	2728	2755	3249	3193	2709	2550	2787	2740	2522	2493	2883	3007	3071	2958	2809	2804
Co	371	375	97	120	362	537	323	325	533	424	183	141	122	212	278	278
Ni	7452	7408	1429	1925	8191	9854	5554	5691	10401	9150	3408	2560	2038	4006	5618	5682
Cu	55	56	21	25	71	72	39	40	77	75	35	34	27	35	48	49
Zn	51	52	57	57	50	48	54	54	49	49	55	57	58	56	54	54
Ga	5.2	5.4	4.1	4.3	5.3	5.6	4.9	5.0	5.1	5.0	4.3	4.0	3.8	4.6	5.6	5.6
Rb	5.4	5.6	4.7	4.4	1.7	1.6	1.27	1.35	1.45	1.54	3.43	4.03	3.17	3.32	4.38	4.22
Sr	8.4	8.5	13.0	13.7	11.4	10.9	12.8	12.6	10.8	11.8	12.1	11.5	12.7	11.9	10.7	10.8
Y	2.6	2.7	3.1	3.1	2.4	2.2	2.7	2.7	2.6	2.6	2.8	2.8	2.8	2.8	2.6	2.6
Zr	6.5	6.5	7.6	7.4	6.8	6.1	7.0	6.8	5.7	6.0	7.0	7.0	7.0	6.9	6.7	6.6
Nb	0.48	0.48	0.55	0.53	0.48	0.43	0.51	0.50	0.44	0.45	0.51	0.52	0.51	0.53	0.50	0.49
Mo	1.48	1.47	0.30	0.39	1.70	2.10	1.05	1.08	1.96	1.77	0.63	0.48	0.38	0.73	1.10	1.10
Cd (ppb)	10.6	9.9	2.6	5.3	5.1	5.6	5.0	5.3	9.9	9.3	9.1	9.4	13.1	13.7	5.1	4.9
Sn	0.30	0.30	0.18	0.19	0.38	0.45	0.28	0.27	0.38	0.39	0.20	0.17	0.17	0.24	0.36	0.31
Sb (ppb)	59.2	58.9	43.9	46.0	76.7	85.9	71.4	64.5	90.5	85.2	43.8	42.3	46.4	60.5	116	88.8
Cs (ppb)	3.54	3.00	3.59	3.25	1.73	1.44	2.12	2.14	1.88	2.17	2.83	2.65	2.70	2.88	3.02	2.87
Ba	3.1	3.0	3.8	3.8	3.3	3.2	3.9	3.9	3.5	3.8	3.8	3.8	3.8	3.8	3.6	3.7
La	0.329	0.334	0.349	0.346	0.264	0.257	0.357	0.355	0.352	0.357	0.361	0.362	0.355	0.350	0.342	0.348
Ce	0.887	0.890	0.954	0.942	0.721	0.693	0.954	0.942	0.939	0.945	0.972	0.960	0.948	0.935	0.920	0.911
Pr	0.127	0.130	0.140	0.136	0.106	0.100	0.138	0.135	0.135	0.136	0.141	0.140	0.137	0.136	0.133	0.133
Nd	0.672	0.675	0.748	0.726	0.556	0.534	0.714	0.705	0.711	0.702	0.730	0.725	0.714	0.705	0.690	0.689
Sm	0.218	0.226	0.252	0.239	0.192	0.179	0.233	0.234	0.231	0.235	0.241	0.237	0.235	0.233	0.227	0.227
Eu	0.076	0.076	0.084	0.086	0.075	0.073	0.094	0.092	0.080	0.088	0.089	0.084	0.087	0.084	0.084	0.081
Gd	0.291	0.289	0.321	0.307	0.247	0.236	0.315	0.312	0.305	0.307	0.316	0.313	0.314	0.307	0.297	0.300
Tb	0.055	0.055	0.061	0.059	0.048	0.046	0.058	0.057	0.056	0.057	0.059	0.058	0.058	0.056	0.056	0.055
Dy	0.369	0.370	0.402	0.397	0.319	0.301	0.391	0.395	0.380	0.388	0.396	0.402	0.396	0.391	0.372	0.378
Ho	0.087	0.087	0.096	0.094	0.075	0.072	0.091	0.091	0.089	0.088	0.092	0.093	0.091	0.090	0.088	0.086
Er	0.256	0.258	0.283	0.279	0.229	0.216	0.271	0.270	0.261	0.264	0.277	0.273	0.273	0.267	0.263	0.261
Yb	0.245	0.243	0.275	0.272	0.227	0.215	0.263	0.263	0.242	0.249	0.263	0.268	0.267	0.259	0.254	0.260
Lu	0.039	0.039	0.044	0.043	0.036	0.034	0.040	0.040	0.038	0.038	0.041	0.042	0.042	0.040	0.040	0.039
Hf	0.169	0.167	0.186	0.178	0.172	0.162	0.176	0.175	0.145	0.154	0.175	0.176	0.171	0.173	0.174	0.171
Ta	0.023	0.023	0.026	0.025	0.023	0.022	0.025	0.024	0.024	0.024	0.025	0.025	0.025	0.025	0.024	0.024
W	0.16	0.16	0.12	0.12	0.18	0.24	0.20	0.19	0.23	0.20	0.26	0.24	0.12	0.17	0.28	0.22
Pb	0.042	0.016	0.029	0.025	0.035	0.036	0.022	0.026	0.053	0.048	0.020	0.018	0.060	0.039	0.021	0.016
Th	0.046	0.047	0.049	0.049	0.041	0.035	0.047	0.046	0.045	0.047	0.047	0.046	0.047	0.046	0.046	0.045
U	0.010	0.011	0.011	0.011	0.009	0.007	0.011	0.011	0.012	0.014	0.012	0.012	0.012	0.011	0.010	0.011

*Data in ppm except as noted.

RESULTS

Lithophile Elements

Refractory lithophile elements in both the impact melt and the host chondrite lithologies of Chico are unfractionated relative to average L-chondrite values (Fig. 2). In the melt rock, absolute concentrations of refractory incompatible lithophile elements such as the rare earth elements (REE) extend to values well above those of average L chondrites, and are negatively correlated with siderophile elements such as Fe, Ni, and Ir (Fig. 3). Vanadium, Zn, and Cr behaved as lithophile elements in the impact melt as shown by their increasing concentrations with decreasing Ni contents (Fig. 4).

Moderately volatile lithophile elements such as K, Rb, Cd, and Zn show considerably more dispersion than the REE (Fig. 2). About half of the dike samples have K contents and K/Ca ratios similar to those of the host chondrite, whereas others are enriched in K, with high K/Ca and K/Na ratios (see also Bogard *et al.*, 1995). On average, K/Na ratios in the melt rocks are higher than those of the host chondrite. Rubidium is enriched in the Chico impact melt compared to the host chondrite and average L chondrites, producing higher Rb/Sr (Fig. 5) as well as lower Ca/K, K/Rb and Ba/Rb ratios. In contrast, the Chico host chondrite is depleted in Rb relative to average L chondrites (Fig. 5).

Notable in the geochemistry of Chico is the profound depletion of Cs and Pb in all samples (Fig. 2). Cesium concentrations are only 1.5 to 3.5 ng/g (Tables 1 and 2; Fig. 6) compared to the average L-chondrite value of 280 ng/g (Wasson and Kallemeyn, 1988). Even using the mean of three determinations of Cs on *bona fide* low shock stage L6 chondrites for normalization (Keays *et al.*, 1971; Walsh and Lipschutz, 1982), Chico is depleted by a factor of ~0.04. Consequently, Rb/Cs ratios in Chico are remarkably high (600–1700 *vs.* the average L-chondrite value of 11; Fig. 6). Lead is also severely depleted in Chico with concentrations ranging from 16 to 60 ng/g compared to 370 ng/g for average L chondrites (Wasson and Kallemeyn, 1988). In contrast to the volatile alkalies, Pb concentrations tend to be lower in the impact melt compared to the host chondrite (Fig. 7).

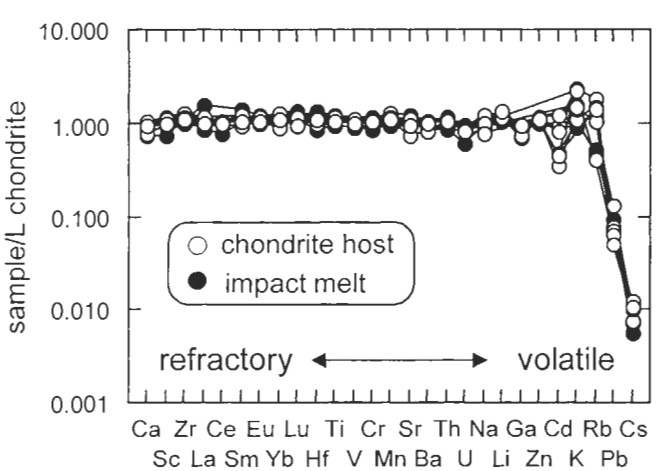

FIG. 2. Composition of the Chico impact melt and host chondrite relative to average L chondrites (normalizing values from Wasson and Kallemeyn, 1988). Refractory lithophile elements in both the impact melt and the Chico host chondrite are unfractionated relative to average L chondrites, with more variability in the moderately and highly volatile elements such as K, Rb, and Cd. Cesium and Pb are severely depleted in all samples of Chico relative to average L chondrites. Using the Cs content of low shock-stage L6 chondrites rather than the L-chondrite mean still indicates severe depletion in Chico (see text).

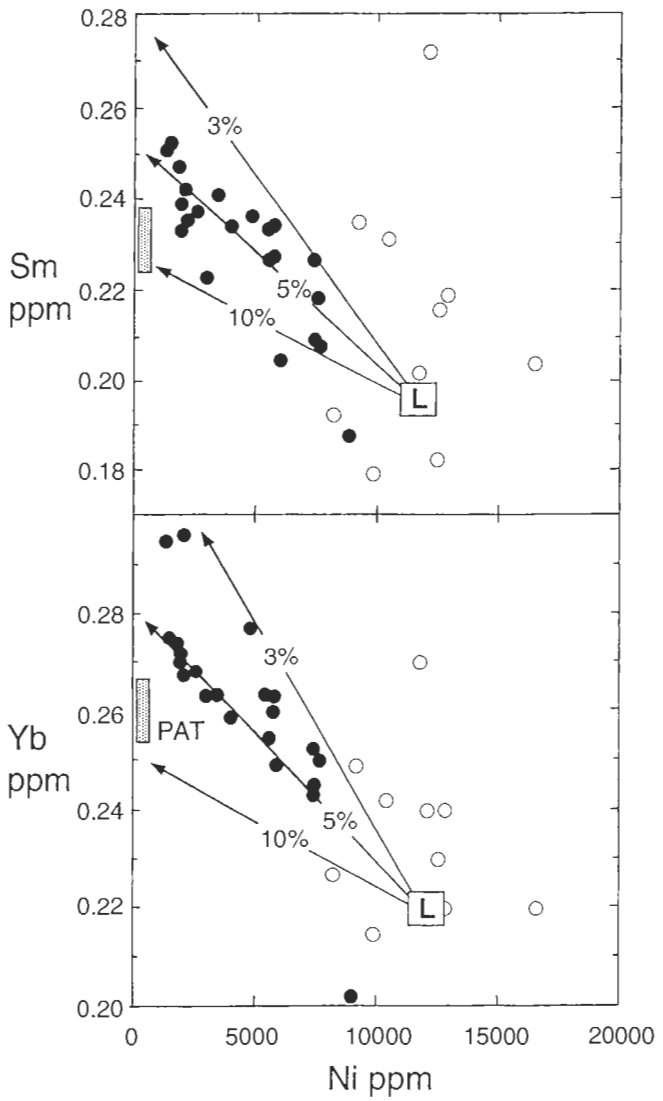

FIG. 3. Samarium and Yb *vs.* Ni concentrations of the Chico and Point of Rocks impact melt (filled circles) and host chondrite (open circles). Lines indicate compositions produced by subtraction of metal with a constant Ni content, indicated by the labels on each line, from an average L-chondrite composition (**L**). The Chico melt rock compositions can be produced by loss of metal plus troilite with an average bulk composition of ~5% Ni. Composition of the PAT 91501 L-chondrite impact melt (hatched rectangle labeled PAT; data from Mittlefehldt and Lindstrom, 2001) implies loss of a metal phase with a somewhat higher bulk Ni content (5–10%). Plot includes ICPMS and INAA data for all analyzed splits (Tables 1 and 2).

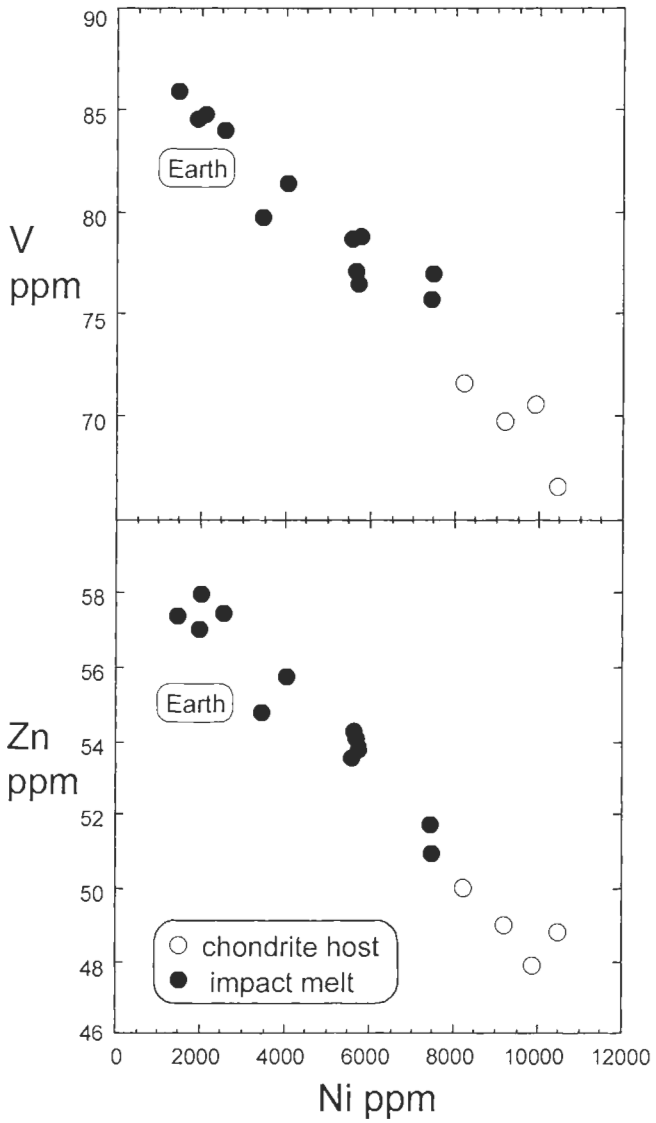

FIG. 4. Vanadium and Zn *vs.* Ni abundances in the Chico impact melt breccia (filled circles) and host chondrite (open circles). Vanadium, Zn, and Cr (not shown) all increase with decreasing Ni content indicating they behaved as lithophile rather than siderophile elements during the impact melting event. Plot includes ICPMS data for all analyzed splits. Earth primitive mantle composition from McDonough and Sun (1995).

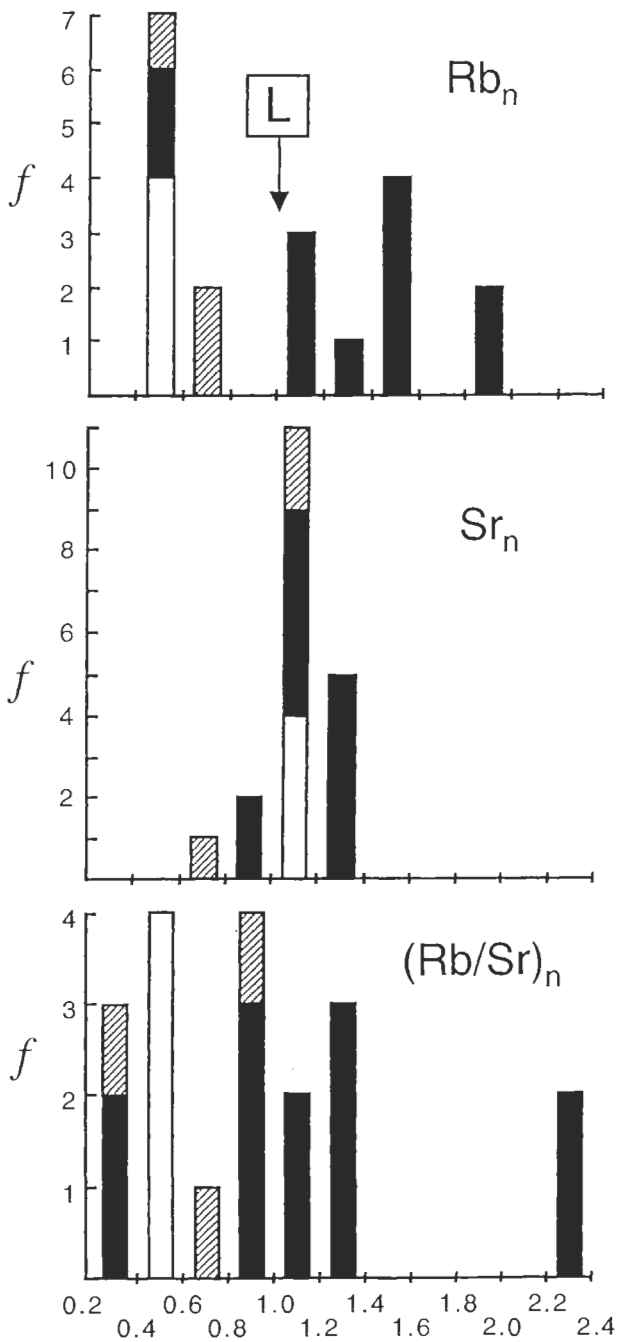

FIG. 5. Histograms of Rb, Sr, and Rb/Sr compositions in the Chico impact melt (filled bars), host chondrite (open bars) and Point of Rocks (stippled bars) normalized to average L chondrites (**L**) and plotted on the same scale. The broad range of Rb compared to Sr reflects redistribution of volatile elements by the 0.5 Ga impact event on the L-chondrite parent body.

Siderophile and Chalcophile Elements

Moderately and highly siderophile elements (Fe, Ni, Co, Ir, Au, As, Cu, Sn, Mo, Ga) in the impact melt span a broad range of concentrations extending from the host chondrite composition to more depleted compositions (Figs. 8 and 9). Siderophile element ratios in the impact melt become increasingly fractionated with loss of metal, as shown by trends to lower Ni/Co, Ir/Ni, Ir/Au, Cu/Ga, Cu/Sn, and higher Se/Co and Cu/Mo ratios with decreasing Ni contents (Fig. 10). The fractionated ratios are not caused by volatility, as Sb/Co and As/Co ratios do not decrease with decreasing Co content as would be expected for thermal mobilization (*e.g.*, Ngo and Lipschutz, 1980). Abundances of FeO* (total Fe calculated as FeO), Ni, Co, Ir, Au, and Se in PAT 91501 fall along extensions of the trends observed for Chico to lower values, reflecting the metal-depleted nature of PAT 91501 relative to Chico (Fig. 8).

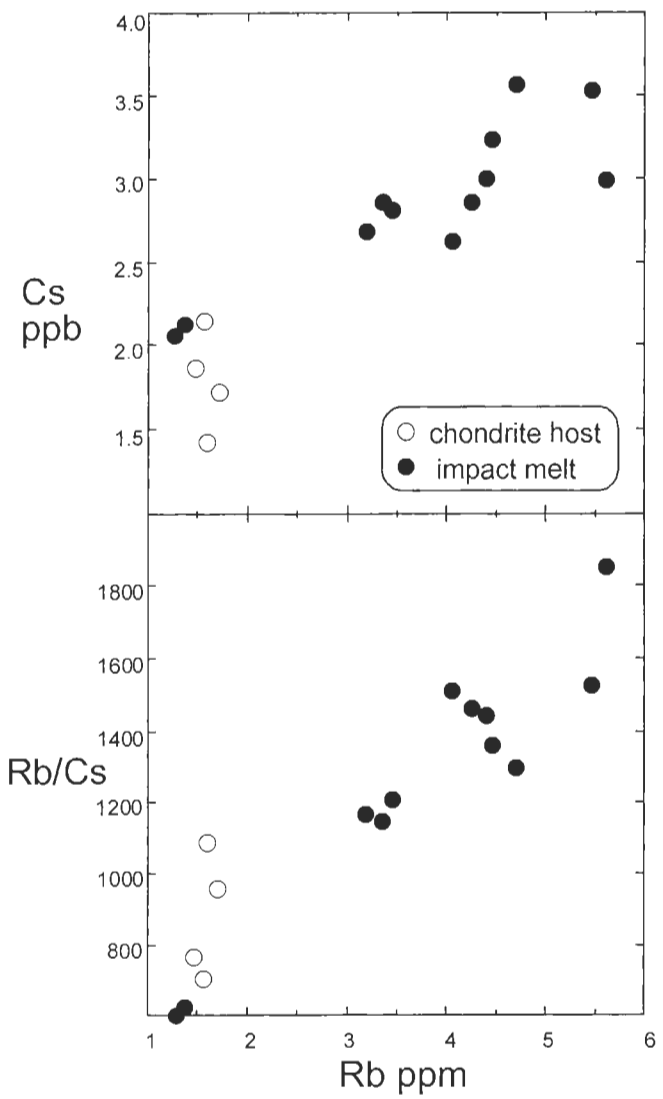

FIG. 6. Cesium concentrations and Rb/Cs ratios *vs.* Rb contents of the Chico impact melt (filled circles) and host chondrite (open circles). Cesium contents in both the impact melt and the host chondrite are severely depleted relative to values typical of ordinary chondrites, resulting in remarkably high Rb/Cs ratios. Plot includes ICPMS data for all analyzed splits.

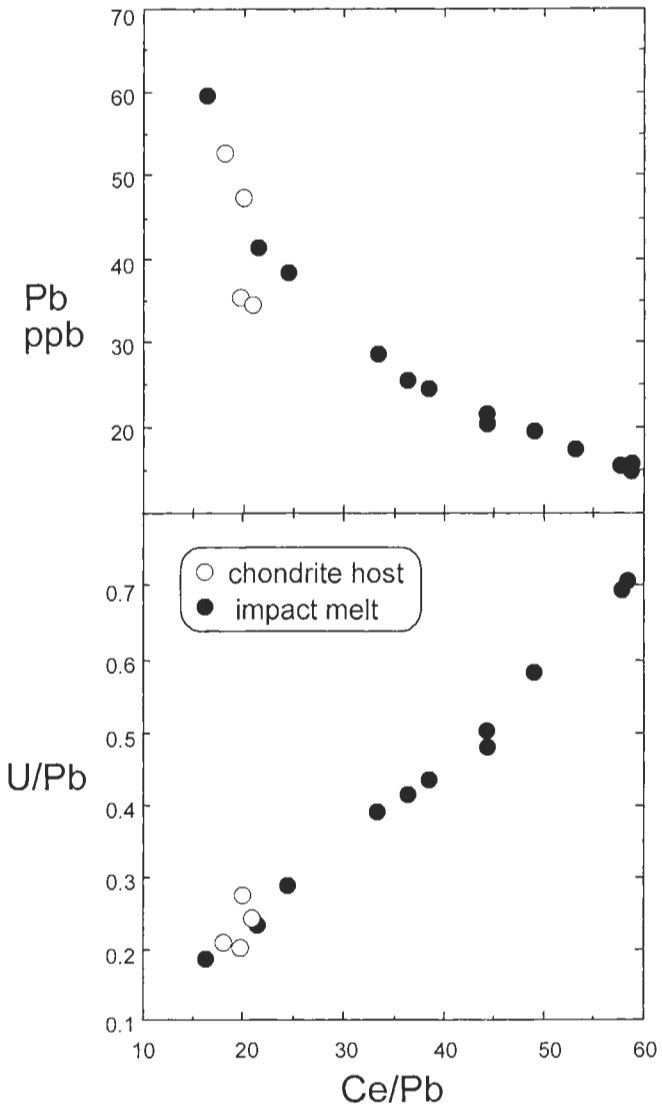

FIG. 7. Ce/Pb ratios *vs.* Pb concentrations and U/Pb ratios in the Chico impact melt (filled circles) and host chondrite (open circles). Lead contents in both the impact melt and the host chondrite are severely depleted relative to values typical of ordinary chondrites, resulting in elevated Ce/Pb and U/Pb ratios. Plot includes ICPMS data for all analyzed splits.

A metal globule separated from the dike (Table 1) has Co, Ni, As and Au contents similar to those of bulk unmelted metal from L5–6 chondrites (Rambaldi, 1976; Kong and Ebihara, 1996), but is enriched in Ir and depleted in Sb. Metal with similar major element compositions (12–14% Ni, 0.3–0.6% P) has been reported previously for the Chico impact melt (Scott *et al.*, 1986) and Shaw (Rambaldi and Larimer, 1976; Taylor *et al.*, 1979). Although Se is depleted in the Chico melt rocks, where it is well correlated with Ni abundances, it was not detected in the metal globule. Selenium is undoubtedly concentrated in the sulfide phase rather than FeNi metal as shown by the high concentration of Se in a troilite nodule from PAT 91501 (172 μg/g; Mittlefehldt and Lindstrom, 2001). Sulfide may have been incompletely sampled when preparing the Chico metal globule for analysis, or it may be heterogeneously distributed. The correlation of Se and Cu (predominantly chalcophile) with Ni (predominantly siderophile) in the melt rocks shows that in general, metal and sulfide are closely associated in the L-chondrite impact melt breccias.

DISCUSSION

Unfractionated refractory lithophile element abundances in both the Chico impact melt and in PAT 91501 (Fig. 3; Mittlefehldt and Lindstrom, 2001) demonstrate virtually complete impact

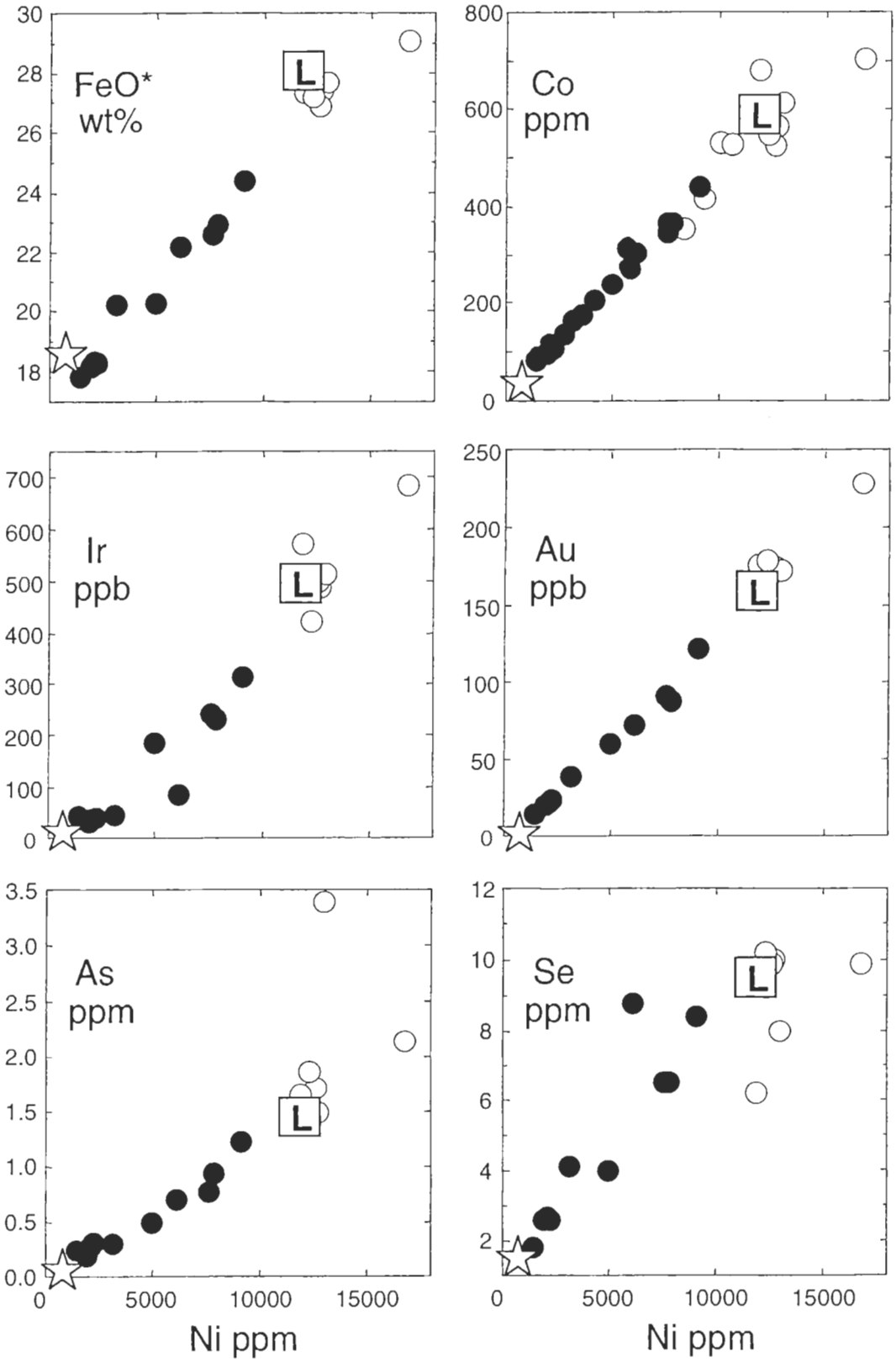

FIG. 8. Concentrations of siderophile and chalcophile elements *vs.* Ni abundances in the Chico, and Point of Rocks impact melt (filled circles), the PAT 91501 impact melt (star), and Chico host chondrite (open circles). Siderophile element abundances in the Chico host chondrite are typical of L chondrites whereas the impact melt is progressively depleted in siderophiles. INAA data for all splits are plotted except for Co concentrations which are INAA and ICPMS data. FeO* is total Fe calculated as FeO. Average composition of L chondrites (**L**) from Wasson and Kallemeyn (1988).

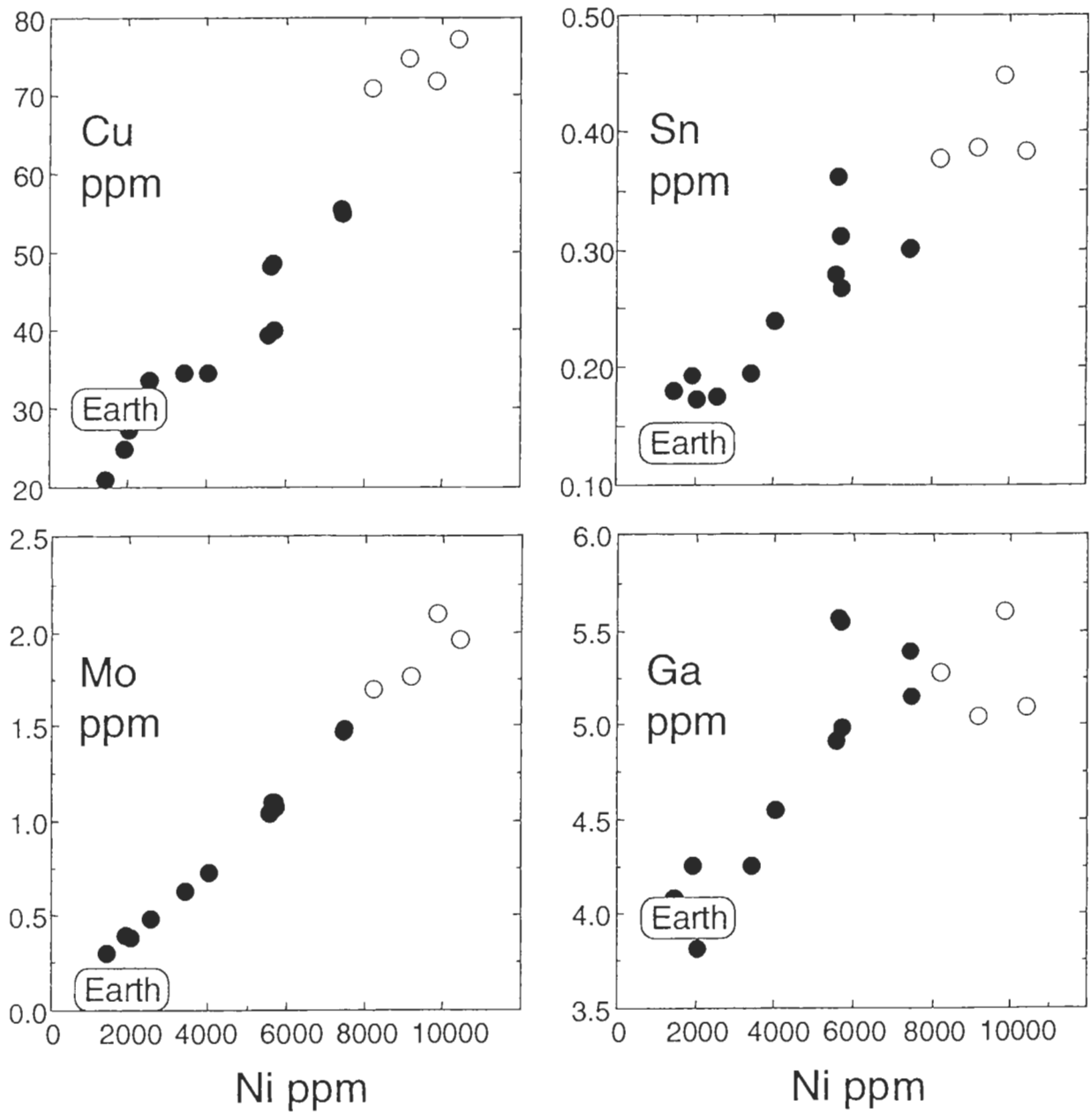

FIG. 9. Concentrations of siderophile and chalcophile elements *vs.* Ni abundances in the Chico, and Point of Rocks impact melt (filled circles), the PAT 91501 impact melt (star), and Chico host chondrite (open circles). Siderophile element abundances in the Chico host chondrite are typical of L chondrites whereas the impact melt is progressively depleted in siderophiles. Data for all splits analyzed by ICPMS are plotted.

melting of the target and negligible crystal-liquid fractionation. The most significant geochemical consequences of the 0.5 Ga impact event on the L-chondrite parent body were: (1) mobilization of moderately and highly volatile elements in the impact melt and the host chondrite, and (2) fractionation of siderophile and chalcophile elements associated with increased metal-silicate heterogeneity in the impact melt. Coarse-grained metal is also evident in the older impact event represented by Shaw (Taylor *et al.*, 1979) suggesting that such features may be relatively common on chondritic planetesimals that have suffered major impact events. In this section we discuss geochemical aspects of the impact-induced volatile element mobility and metal-silicate fractionation in Chico and other L chondrites.

Volatile Element Fractionation in L Chondrites by Impacts

Systematic variations of element ratios that emphasize relative volatilities (e.g., K/Na, K/Rb, Rb/Cs, Rb/Sr, Ce/Pb,

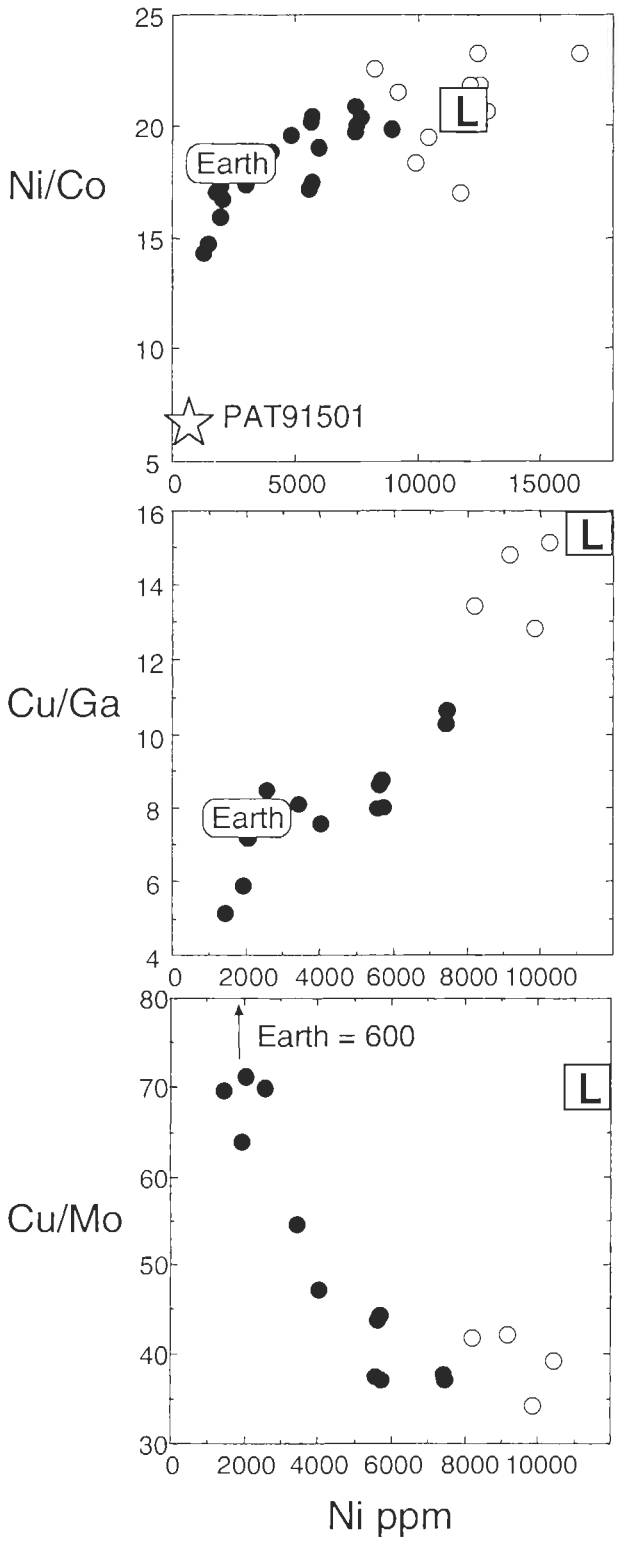

FIG. 10. Siderophile and chalcophile element ratios (Ni/Co, Cu/Ga, Cu/Sn) *vs.* Ni abundances in the Chico impact melt (filled circles), PAT 91501 (star) and Chico host chondrite (open circles). Loss of metal fractionated siderophile and chalcophile element ratios in the L-chondrite impact melt. Average composition of L chondrites (L) from Wasson and Kallemeyn (1988). Earth primitive mantle compositions from McDonough and Sun (1995).

U/Pb; Figs. 5, 6, and 7) provide clear evidence for differential mobility of moderately and highly volatile elements in the L-chondrite impact melt breccias, and the Rb-Sr internal isochron ages for Chico and Point of Rocks (Nakamura *et al.*, 1990; Fujiwara and Nakamura, 1992) link this fractionation to the 0.5 Ga impact event. Volatile element redistribution by this event did not simply involve migration from the hot impact melt into the cooler host chondrite, however, as K and Rb contents of the Chico impact melt are mostly greater than average L chondrites, whereas the Chico host chondrite and the Point of Rocks impact melt (Nakamura *et al.*, 1990) are depleted in K and Rb, with K/Ca and Rb/Sr ratios lower than average L chondrites (Fig. 5). In PAT 91501, Na and K are highly variable in melt inclusions, interstitial glass, and bulk rock samples although K/Ca and K/Na ratios of bulk rock splits of PAT 91501 are within uncertainty the same as those of average L chondrites (Mittlefehldt and Lindstrom, 2001).

The 0.5 Ga impact event apparently created significant alkali element heterogeneity on the L-chondrite parent body, with K and Rb being mobilized and redistributed to both higher and lower values around the average L-chondrite composition. This contrasts with the relatively constant abundance of more refractory lithophile elements such as Ca and Sr (Fig. 5), and shows that the variation in K and Rb contents cannot be due to a process such as heterogeneous distribution of glass (which would contain most of the Rb and Sr, and presumably a relatively constant Rb/Sr), or dilution with a phase such as olivine or pyroxene (which would not fractionate Rb from Sr). Impact-induced thermal volatility appears to be the best explanation for the broad range of moderately volatile element abundances in the L-chondrite melt breccias.

In contrast to the other alkalies, Cs is profoundly depleted in all samples of Chico compared to average L chondrites (Fig. 2). Our mean host chondrite value (samples 3A, 3B, 6A, 6B, Table 2) is 1.8 ng/g and the mean impact melt value is 2.9 ng/g. These are among the lowest reported for L chondrites (Huston and Lipschutz, 1984; Keays *et al.*, 1971; Neal *et al.*, 1981; Walsh and Lipschutz, 1982) and represent nearly quantitative (99%) loss of Cs from Chico relative to average L-chondrite compositions (280 ng/g; Wasson and Kallemeyn, 1988). Somewhat counter-intuitively, Rb/Cs ratios in Chico correlate positively with both Rb and Cs contents. This is opposite to the sense expected for volatility-related fractionation which predicts preferential loss of more volatile Cs and higher Rb/Cs ratios in the most depleted samples. Cesium contents in Chico are relatively constant and may reflect a lower limit of Cs depletion at about 2–3 ng/g with less volatile Rb showing more variation and controlling the measured Rb/Cs ratio. Similar trends of alkali depletion have been produced experimentally by heating lunar breccias (Gibson and Hubbard, 1972, 1973).

Other highly mobile elements such as Pb, Cd, Tl, and Bi are also depleted in both the impact melt and the host chondrite lithologies in Chico (Fig. 2; Yolcubal *et al.*, 1997), as is Br in

PAT 91501 (Mittlefehldt and Lindstrom, 2001). Lead abundances in Chico are consistent with ~90% loss from an average L chondrite. Ratios of U/Pb and Ce/Pb in Chico are high relative to values for average L chondrites and are even greater than those of the volatile-depleted terrestrial mantle: U/Pb = 0.22–0.61 and Ce/Pb = 18–50 for Chico compared to values of 0.14 and 11.2, respectively for Earth's primitive mantle (McDonough and Sun, 1995). Extreme (90–99%) losses of highly volatile elements imply a highly efficient fractionation and transport process possibly involving a vapor or fluid phase.

Moderately and highly mobile element abundances in L chondrites show a significant range of concentrations that broadly correlates with shock facies (as defined by Dodd and Jarosewich, 1979), and with noble gas abundances (Smales *et al.*, 1964; Tandon and Wasson, 1968; Keays *et al.*, 1971; Neal *et al.*, 1981; Walsh and Lipschutz, 1982; Huston and Lipschutz, 1984). L chondrites tend to show decreasing concentrations of mobile trace elements such as Cs, In, Cd, Tl, and Bi with increasing shock intensity, although this general correlation is not always evident in every sample. For example, the L6 chondrite Orvinio is highly shocked and yet has elevated Rb and Cs contents, and some heavily shocked L chondrites are enriched in elements such as Cs, Br, and Tl relative to less volatile elements, with abundances occasionally exceeding CI values (Keays *et al.*, 1971; Walsh and Lipschutz, 1982). The wide range of alkali element compositions in Chico and Point of Rocks (Fig. 5) shows that volatile element heterogeneity is to be expected for chondritic planetesimals that experienced major impact events.

Early studies emphasized correlations between petrologic grade and volatile element abundance (Tandon and Wasson, 1968; Keays *et al.*, 1971), but there appears to be a better correlation between volatile element depletion and shock intensity in the L chondrites than with petrologic type or predictions of condensation models (Smales *et al.*, 1964; Keays *et al.*, 1971; Walsh and Lipschutz, 1982; Huston and Lipschutz, 1984). Fractionation and depletion of moderately and highly volatile elements by impacts is a more likely explanation for their wide variations in many L chondrites than either parent-body metamorphism or mixing of nebular components.

Numerous volatilization experiments on chondritic and lunar samples have shown that the pattern of element mobility produced by impact heating differs from that expected for condensation from a solar nebula (Smales *et al.*, 1964; Gibson and Hubbard, 1972, 1973; Wulf *et al.*, 1995; Walsh and Lipschutz, 1982). For example, Pb appears to be more volatile during subsolidus heating than predicted for condensation possibly due to decomposition of sulfides (Silver, 1972; Wulf *et al.*, 1995). Alkali loss during heating also produces large fractionations of Na/K, K/Rb and Rb/Cs in chondrites and lunar breccias (Gibson and Hubbard, 1972, 1973; Walsh and Lipschutz, 1982; Huston and Lipschutz, 1984; Wulf *et al.*, 1995) whereas the similar condensation temperatures for K, Rb, and Cs (942–967 K; Allegre *et al.*, 2001), make it unlikely that fractional condensation would produce large variations in the relative abundances of these elements. Evaporation under reducing conditions seems to be especially effective for mobilizing alkalies in chondritic materials (Wulf *et al.*, 1995). The pattern of K and Rb redistribution coupled with the severe depletion of more volatile elements such as Cs and Pb in Chico and the other L-chondrite impact breccias suggests mobilization of these elements under either relatively modest peak temperatures, perhaps about 800–1000 °C, or during a geologically brief heating interval.

Metal-Silicate Fractionation in the Impact Melt

Another significant consequence of the 0.5 Ga impact event on the L-chondrite parent body was the agglomeration of coarse-grained metal in the impact melt. Size of the metal phase is one of the most important controls on the effectiveness of metal-silicate segregation during either static melting of planets and asteroids, or percolation of metal through a deforming matrix. This in turn may influence the extent of siderophile element equilibrium between metal and silicate (Stevenson, 1990; Taylor, 1992). Impacts probably were not the primary heat source driving planetary differentiation (Keil *et al.*, 1997), but they may have contributed to the production of coarse-grained metal and increased metal-silicate heterogeneity within planetesimals. The combination of high strain rates and extensive melting engendered by a sizable impact event would enhance the physical separation of metal from silicate, and the development of shock-induced fractures may help channel the mobilized metal and sulfide (Rushmer *et al.*, 2000).

At least two collisional events on the L-chondrite parent body produced an increase in the scale of metal-silicate heterogeneity in impact melt breccias (>10–100 mm) relative to the host chondrite (<0.1–1 mm). In Chico, molten metal + sulfide globules were extracted from a 30 cm wide zone of impact melt and concentrated along the axis of the dike (Bogard *et al.*, 1995). In Shaw and PAT 91501, centimeter-sized metal sulfide globules typically are separated by several centimeters (Taylor *et al.*, 1979; Mittlefehldt and Lindstrom, 2001). A natural consequence of impact melting on chondritic asteroids appears to be the production of coarser grained, igneous metal from finer grained chondritic precursors. As collisions between chondritic planetesimals would have been relatively common during accretion, such events may have contributed to an early generation of coarse-grained metal within colliding planetesimals. Large impacts may have created sufficient metal-silicate heterogeneity in asteroids to be detectable spectroscopically.

Increased metal-silicate heterogeneity in the Chico impact melt is also apparent in the geochemical data. The host chondrite is relatively (although not perfectly) homogeneous on an ~3 mm scale (the approximate linear dimension of our

50 mg INAA samples) and similar in composition to average L chondrites. In contrast, the impact melt is both more heterogeneous and systematically depleted in siderophile elements when sampled at the same scale as the host chondrite. This compositional variability is seen most clearly in the Ni, Co, and Ir contents of some duplicate samples which are outside of instrumental precision and vary by almost a factor of 2 among samples with masses of ~100 mg (*e.g.*, ICPMS data for melt sample 8; Tables 1, 2), reflecting small differences in the content or composition of metal. The smaller handpicked samples analyzed by INAA show a greater range of Ni and Co contents than do the larger homogenized samples analyzed by ICPMS, consistent with more representative sampling of metal in the latter. Compositional variability at this scale is a natural result of internal heterogeneity in these rocks (Haas and Haskin, 1991).

Details of the metal-silicate fractionation are shown in Fig. 11, a plot of L-chondrite-normalized Se/Co *vs.* Ir/Ni based on our INAA data. This diagram qualitatively illustrates the effects of melting in the Fe–Ni–S system for Acapulco- and Lodran-like achondrites (Mittlefehldt *et al.*, 1996), and is applied here to the L-chondrite impact melts. Melting in the L-chondrite Fe–Ni–S system will commence along the alloy-sulfide cotectic, and the first phase to completely melt will be troilite. Selenium is a chalcophile element and will be quantitatively partitioned into the sulfide melt. Iridium is a highly compatible siderophile element, and will be strongly enriched in the solid metal alloy

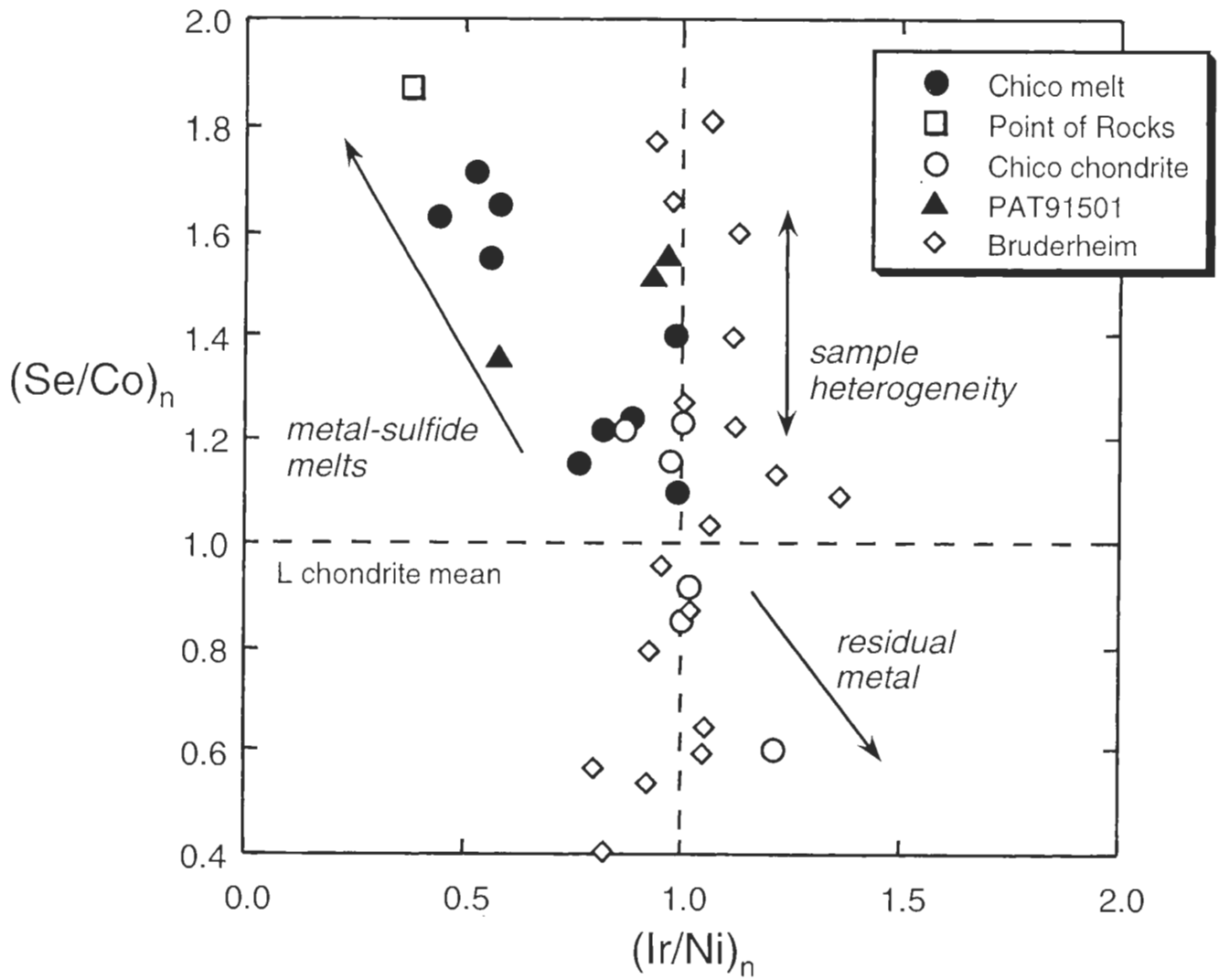

FIG. 11. L-chondrite-normalized Se/Co *vs.* Ir/Ni ratios for the Chico impact melt (filled circles) and host chondrite (open circles), together with L-chondrite impact melt from Point of Rocks (open square, this work) and PAT 91501 (filled triangles; Mittlefehldt and Lindstrom, 2001). For comparison, a subset of the data obtained by Haas and Haskin (1991) for ~100 mg chips of the Bruderheim L6 chondrite is also shown (open diamonds; some of their data extend to lower and higher Se/Co ratios). L-chondrite mean is from Wasson and Kallemeyn (1988).

whereas Ni and Co will be less strongly enriched in the solid metal. Hence, either partial melting or fractional crystallization in the chondritic metal–troilite system will result in a sulfide-rich melt phase with high Se/Co and low Ir/Ni, and solid FeNi metal with the opposite characteristics. Troilite from PAT 91501 has the low Ir/Ni and high Se/Co predicted by this model (Mittlefehldt and Lindstrom, 2001) and the sulfide-poor metal globule from Chico has the expected high Ir/Ni (Table 1).

The Chico data show two distinct trends on Fig. 11. Samples of the chondritic host material predominantly show variable Se/Co and approximately L-chondritic Ir/Ni ratios. One or two Chico melt samples and two of the PAT 91501 melt samples also follow this trend which is consistent with simple heterogeneous distribution of metal (Haas and Haskin, 1991). Indeed, our samples of Chico host chondrite fall within the rather broad range of data obtained on ~100 mg sized samples of the Bruderheim L6 chondrite (Haas and Haskin, 1991). One sample of the Chico host chondrite with a low Se content, low Se/Co, and slightly higher Ir/Ni than mean L chondrites may have lost a fraction of Fe-Ni-S melt. Some splits of Bruderheim also have low Se/Co ratios, but all of these have unusually high Co contents rather than low Se contents. The second trend on Fig. 11, populated by melt samples from Chico, Point of Rocks, and PAT 91501, has increasing Se/Co ratios and decreasing Ir/Ni ratios. This trend is qualitatively consistent with incorporation or preferential retention of small amounts of sulfide-rich melt into metal-depleted portions of the impact melt.

The complexity of metal-silicate fractionation processes that can occur during impact melting of chondritic planetesimals is evident from the correlation between siderophile and lithophile elements in the Chico impact melt. Incompatible lithophile elements such as the REE correlate inversely with Ni abundance in the Chico impact melt. One possible cause for this is an increase in incompatible lithophile element contents in the residual silicate melt by removal of metal. However, the observed REE concentrations cannot be produced simply by loss of metal with 13% Ni (measured composition of the metal globule separated from the dike; Table 1), as this would deplete Ni too rapidly and produce Sm and Yb concentrations lower than are observed at a given Ni content (Fig. 3). Alternatively, loss of metal plus troilite with an average bulk composition of 5% Ni produces a better fit to the Ni-Sm-Yb trends for Chico. The compositions for PAT 91501 fall between the trends expected for loss of metal plus troilite with 5–10% Ni (Fig. 3). As discussed above, the immiscible metal + troilite globules observed in the Chico impact melt would be expected to have bulk Ni contents lower than that of pure FeNi metal, in qualitative agreement with the Ni-Sm-Yb trends. Variable composition of the metal phase during crystallization of the impact melt may also explain these trends. Additional studies of metal and sulfide compositions in Chico are needed to evaluate these possibilities.

Siderophile Element Distribution Coefficients: Inefficient Separation of Metal

Metal-silicate fractionation during impact melting is not necessarily an equilibrium process. Moderately and highly siderophile elements are systematically depleted in the Chico impact melt relative to host chondrite in the samples analyzed here. However, siderophile element concentrations in the Chico and PAT 91501 impact melts imply surprisingly small effective bulk metal/silicate distribution coefficients ($D_{metal/silicate}$ = concentration of an element in the metal fragment/concentration of that element in the most metal-depleted sample of impact melt). $D_{metal/silicate}$ values inferred for the Chico impact melt are on the order of 10^2 for Ni, Co, Ir and Au (Table 1) rather than $\geq 10^{3-6}$ as expected from experimental measurements of low-pressure metal-silicate equilibrium (Righter *et al.*, 1997; Walter *et al.*, 2000 and references therein). Mass balance calculations assuming metal with a Ni content similar to that observed in Shaw and the fragment separated from the Chico impact melt (*i.e.*, 13%, Table 1 and Taylor *et al.*, 1979) are consistent with relatively small $D_{metal/silicate}$ values.

The unusually low effective $D_{metal/silicate}$ values in the Chico impact melt are plausibly related to incomplete segregation of metal during crystallization of the melt. Small blebs of metal adhering to silicate crystals are apparent in backscattered electron images of the impact melt (Fig. 1) demonstrating incomplete separation of metal from the silicate during crystallization. The amount of retained metal appears to be <<1% based on petrographic observations. Notable is the relatively inefficient extraction of siderophile elements despite almost total melting of the silicates and presumably high shear stresses during injection of the dike. High temperatures associated with impact melting, and the ultramafic (chondritic) bulk composition of the Chico impact melt may also have contributed to the low effective bulk $D_{metal/silicate}$ values (Righter *et al.*, 1997).

Inefficient segregation of metal has been proposed as a plausible explanation of the unexpectedly high concentrations of siderophile elements in the terrestrial mantle (Jones and Drake, 1986). Although the relatively small (1–10 cm) lengthscale of metal-silicate heterogeneity in the L-chondrite impact melts renders a direct comparison with core formation problematic, here we compare the siderophile element characteristics of these breccias with those of the Earth's upper mantle to place the results in a familiar context. Concentrations of several siderophile and chalcophile elements, including Ni, Co, Cu, Sn, and Ga, in the melt breccias extend to values similar to those of the Earth's upper mantle (Fig. 9), as do certain siderophile element ratios such as Ni/Co and Cu/Ga (Fig. 10). However, other highly and moderately siderophile or chalcophile elements (*e.g.*, Ir, Au, Mo, As, Se) are overabundant in the L-chondrite impact melt compared to the terrestrial mantle. For example, the most metal-depleted samples of Chico

impact melt have Ni contents similar to terrestrial peridotites (Figs. 9 and 10) but ≥10× more Ir (45–50 ppb *vs.* 3 ppb; terrestrial mantle values from McDonough and Sun, 1995). Although PAT 91501 has Ni contents significantly lower than the terrestrial mantle (~450 *vs.* 2000 ppm, respectively), the Ir content of PAT 91501 (9.2–17.9 ppb; Mittlefehldt and Lindstrom, 2001), is still a factor of 3–5× greater than that of terrestrial peridotites.

The classic "excess siderophile" problem (Ringwood, 1966; Brett, 1971; Chou, 1978; Jagoutz *et al.*, 1979; Morgan, 1986; Righter *et al.*, 1997) appears to be more severe in the L-chondrite impact melts than it is in the Earth's upper mantle. Siderophile element partition coefficients are complex functions of T, P, fO_2, and melt composition (Righter *et al.*, 1997) but even under extreme conditions it is difficult to produce equilibrium distribution coefficients as small as 10^2 for highly siderophile elements such as Ir. Excess concentrations of siderophile elements beyond those expected from low-pressure equilibrium partitioning would be expected for imperfect segregation of metal from a crystallizing silicate melt, and a similar process might have influenced the siderophile element composition of planetary mantles if they were partially molten during the later stages of accretion (Jones and Drake, 1986). Inefficient metal-silicate segregation may have been more likely in the terrestrial upper mantle if it was partially molten at the time the late veneer was added, such as might have been the case if the Moon-forming mega-impact happened when the protoearth was about 50–70% of its present size (Ringwood, 1989; Cameron and Canup, 1999).

CONCLUSIONS

An energetic collision at 0.5 Ga shocked and melted portions of the L-chondrite parent body. The Chico L-chondrite is an impact melt breccia produced by this event. Geochemical effects of this collision reflected in Chico include fractionation of siderophile, chalcophile, and moderately volatile lithophile elements due to metal-silicate segregation and thermal volatility. In contrast, refractory lithophile elements in the impact melt are identical to average L chondrites, indicating near-total fusion of the chondritic target and negligible crystal-liquid fractionation during emplacement of the melt. Variable alkali element compositions and striking depletions of moderately and highly mobile elements such as Cs and Pb in Chico and other L chondrites are more consistent with redistribution and loss of these elements by impact heating rather than a primary nebular process. Impact melting contributed to a coarsening of metal and increased lengthscale of metal-silicate heterogeneity. Effective bulk metal/silicate-melt distribution coefficients for siderophile elements in the Chico impact melt are surprisingly small (~10^2), likely due to inefficient extraction of metal even at high silicate melt fractions. Impact processing may have played an important role in modifying the primary distributions volatile and siderophile elements in chondritic planetesimals.

Acknowledgements–This work was supported by the Lunar and Planetary Institute, NASA JSC, the Australian Research Council, and NASA RTOP # 152-13-40-12 to M. M. Lindstrom. Thanks to Klaus Keil, Ed Scott and Don Bogard for their introduction to Chico. Journal reviews by Kevin Righter and Alex Ruzicka, and comments by Paul Warren are appreciated.

Editorial handling: P. H. Warren

REFERENCES

ALLEGRE C., MANHES G. AND LEWIN E. (2001) Chemical composition of the Earth and the volatility control on planetary genetics. *Earth Planet. Sci. Lett.* **185**, 49–69.

BREARLEY A. J AND JONES R. H. (1998) Chondritic meteorites. In *Planetary Materials* (ed. J. J. Papike), pp. 3-1 to 3-398. Reviews in Mineralogy **36**, Mineralogical Society of America, Washington, D.C., USA.

BRETT R. (1971) The Earth's core: Speculations on its chemical equilibrium with the mantle. *Geochim. Cosmochim. Acta* **35**, 203–221.

BOGARD D. D. AND HIRSCH W. C. (1980) ^{40}Ar-^{39}Ar dating, Ar diffusion properties, and cooling rate determinations of severely shocked chondrites. *Geochim. Cosmochim. Acta* **44**, 1667–1682.

BOGARD D. D., GARRISON D. H., NORMAN M., SCOTT E. R. D. AND KEIL K. (1995) ^{39}Ar-^{40}Ar age and petrology of Chico: Large scale impact melting on the L chondrite parent body. *Geochim. Cosmochim. Acta* **59**, 1383–1399.

CAMERON A. G. W. AND CANUP R. M. (1999) State of the protoearth following the giant impact (abstract). *Lunar Planet Sci.* **30**, #1150, Lunar and Planetary Institute, Houston, Texas, USA (CD-ROM).

CHOU C-L. (1978) Fractionation of siderophile elements in the Earth's upper mantle. *Proc. Lunar Planet. Sci. Conf.* **9th**, 219–230.

DODD R. T. AND JAROSEWICH E. (1979) Incipient melting in and shock classification of L-group chondrites. *Earth Planet. Sci. Lett.* **44**, 335–340.

FUJIWARA T. AND NAKAMURA N. (1992) Additional evidence of a young melting event on the L-chondrite parent body (abstract). *Lunar Planet. Sci.* **23**, 387–388.

GARRISON D. H., BOGARD D. D., ALBRECHT A. A., VOGT S., HERZOG G. F., KLEIN J., FINK D., DEZFOULY-ARJOMANDY B. AND MIDDLETON R. (1992) Cosmogenic nuclides in core samples of the Chico L6 chondrite: Evidence for irradiation under high shielding. *Meteoritics* **27**, 371–381.

GIBSON E. K. AND HUBBARD N. J. (1972) Thermal volatilization studies on lunar samples. *Proc. Lunar Sci. Conf.* **3rd**, 2003–2014.

GIBSON E. K., HUBBARD N. J., WIESMANN H., BANSAL B. M. AND MOORE G. W. (1973) How to lose Rb, K, and change the K/Rb: An experimental study. *Proc. Lunar Planet. Sci. Conf.* **4th**, 1263–1274.

HAACK H., FARINELLA P., SCOTT E. R. D. AND KEIL K. (1996) Meteoritics, asteroidal, and theoretical constraints on the 500 Ma disruption of the L chondrite parent body. *Icarus* **119**, 182–191.

HAAS J. R. AND HASKIN L. A. (1991) Compositional variations among whole-rock fragments of the L6 chondrite Bruderheim. *Meteoritics* **26**, 13–26.

HARVEY R. P. AND ROEDDER E. (1994) Melt inclusions in PAT 91501: Evidence for crystallization from an L chondrite impact melt (abstract). *Lunar Planet. Sci.* **25**, 513.

HUSTON T. J. AND LIPSCHUTZ M. E. (1984) Chemical studies of L chondrites–III. Mobile elements and ^{40}Ar/^{39}Ar ages. *Geochim. Cosmochim. Acta* **48**, 1319–1329.

JAGOUTZ E., PALME H., BADDENHAUSEN H., BLUM K., CENDALES M., DREIBUS G., SPETTEL B., LORENZ V. AND WÄNKE H. (1979) The abundances of major, minor and trace elements in the Earth's

mantle as derived from primitive ultramafic nodules. *Proc. Lunar Planet Sci. Conf.* **10th**, 2031–2050.

JONES J. H. AND DRAKE M. J. (1986) Geochemical constraints on core formation in the Earth. *Nature* **322**, 221–228.

KEAYS R. R., GANAPATHY R. AND ANDERS E. (1971) Chemical fractionations in meteorites–IV. Abundances of fourteen trace elements in L-chondrites; implications for cosmothermometry. *Geochim. Cosmochim. Acta* **35**, 337–363.

KEIL K., STÖFFLER D., LOVE S. G. AND SCOTT E. R. D. (1997) Constraints on the role of impact heating and melting in asteroids. *Meteorit. Planet. Sci.* **32**, 349–363.

KONG P. AND EBIHARA M. (1996) Metal phases of L chondrites: Their formation and evolution in the nebula and in the parent body. *Geochim. Cosmochim. Acta* **60**, 2667–2680.

LA PAZ L. (1954) Preliminary note on the Chico, New Mexico, aerolite (CN = 1042,365). *Meteoritics* **1**, 182–186.

MARTI K. AND GRAF T. (1992) Cosmic-ray exposure history of ordinary chondrites. *Ann. Rev. Earth Planet. Sci.* **20**, 221–243.

MCDONOUGH W. F. AND SUN S-S. (1995) The composition of the Earth. *Chem. Geol.* **120**, 223–253.

MITTLEFEHLDT D. W. AND LINDSTROM M. M. (1993) Geochemistry and petrology of a suite of ten Yamato HED meteorites. *Proc. NIPR Symp. Antarctic Meteorites* **6**, 268–292.

MITTLEFEHLDT D. W. AND LINDSTROM M. M. (2001) Petrology and geochemistry of Patuxent Range 91501, a clast-poor impact melt from the L chondrite parent body and Lewis Cliff 88663, an L7 chondrite. *Meteorit. Planet. Sci.* **37**, 439–458.

MITTLEFEHLDT D. W., LINDSTROM M. M., BOGARD D. D., GARRISON D. H. AND FIELD S. W. (1996) Acapulco- and Lodran-like achondrites: Petrology, geochemistry, chronology and origin. *Geochim. Cosmochim. Acta* **60**, 867–882.

MORGAN J. W. (1986) Ultramafic xenoliths: Clues to Earth's late accretionary history. *J. Geophys. Res.* **91**, 12 375–12 387.

NAKAMURA N., FUJIWARA T. AND NOHDA S. (1990) Young asteroid melting event indicated by Rb-Sr dating of Point of Rocks meteorite. *Nature* **345**, 51–53.

NEAL C. W., DODD R. T., JAROSEWICH E. AND LIPSCHUTZ M. E. (1981) Chemical studies of L-chondrites–I. A study of possible chemical sub-groups. *Geochim. Cosmochim. Acta* **45**, 891–898.

NGO H. T. AND LIPSCHUTZ M. E. (1980) Thermal metamorphism of primitive meteorites–X. Additional trace elements in Allende (C3V) heated to 1400 °C. *Geochim. Cosmochim. Acta* **44**, 731–739.

NORMAN M. D., GRIFFIN W. L., PEARSON N. J., GARCIA M. O. AND O'REILLY S. Y. (1998) Quantitative analysis of trace element abundances in glasses and minerals: A comparison of laser ablation ICPMS, solution ICPMS, proton microprobe, and electron microprobe data. *J. Anal. At. Spectrom.* **13**, 477–482.

RAMBALDI E. R. (1976) Trace element content of metals from L-group chondrites. *Earth Planet. Sci. Lett.* **31**, 224–238.

RAMBALDI E. R. AND LARIMER J. W. (1976) The Shaw chondrite, I. The case of the missing metal. *Earth Planet. Sci. Lett.* **33**, 61–66.

RIGHTER K., DRAKE M. J. AND YAXLEY G. (1997) Prediction of siderophile element metal-silicate partition coefficients to 120 kb and 2800 °C: The effect of pressure, temperature, fO_2 and silicate and metallic melt composition. *Phys. Earth Planet. Interiors* **100**, 115–134.

RINGWOOD A. E. (1966) Chemical composition of the terrestrial planets. *Geochim. Cosmochim. Acta* **30**, 41–104.

RINGWOOD A. E. (1989) Flaws in the giant impact hypothesis of lunar origin. *Earth Planet. Sci. Lett.* **95**, 208–214.

RUBIN A. E. (1985) Impact melt products of chondritic material. *Rev. Geophys.* **23**, 277–300.

RUSHMER T., MINARIK W. G. AND TAYLOR G. J. (2000) Physical processes of core formation. In *Origin of the Earth and Moon* (eds. R. Canup and K. Righter), pp. 227–243. Lunar and Planetary Institute and University of Arizona Press, Tucson, Arizona, USA.

SCOTT E. R. D., MAGGIORE P., TAYLOR G. J., KEIL K. AND SZUWALSKI D. (1986) Chondritic impact melts and cratering processes on asteroids (abstract). *Lunar Planet. Sci.* **17**, 785–786.

SILVER L. T. (1972) Lead volatilization and volatile element transfer processes on the Moon (abstract). *Lunar Sci.* **3**, 701–703.

SMALES A. A., HUGHES T. C., MAPPER D., MCINNES C. A. J. AND WEBSTER R. K. (1964) The distribution of rubidium and caesium in stony meteorites by neutron activation analysis and by mass spectrometry. *Geochim. Cosmochim. Acta* **28**, 209–233.

STEVENSON D. J. (1990) Fluid dynamics of core formation. In *Origin of the Earth* (eds. H. E. Newsom and J. H. Jones), pp. 231–249. Oxford Univ. Press, New York, New York, USA.

STÖFFLER D., KEIL K. AND SCOTT E. R. D. (1991) Shock metamorphism of ordinary chondrites. *Geochim. Cosmochim. Acta* **55**, 3845–3867.

TANDON S. N. AND WASSON J. T. (1968) Gallium, germanium, indium, and iridium variations in a suite of L-chondrites. *Geochim. Cosmochim. Acta* **32**, 1087–1109.

TAYLOR G. J. (1992) Core formation in asteroids. *J. Geophys. Res.* **97**, 14 717–14 726.

TAYLOR G. J., KEIL K., BERKLEY J. L., LANGE D. E., FODOR R. V. AND FRULAND R. M. (1979) The Shaw meteorite: History of a chondrite consisting of impact-melted and metamorphic lithologies. *Geochim. Cosmochim. Acta* **43**, 323–337.

WALSH T. M. AND LIPSCHUTZ M. E. (1982) Chemical studies of L chondrites–II. Shock-induced trace element mobilization. *Geochim. Cosmochim. Acta* **46**, 2491–2500.

WALTER M. J., NEWSOM H. E., ERTEL W. AND HOLZHEID A. (2000) Siderophile elements in the Earth and Moon: Metal/silicate partitioning and implications for core formation. In *Origin of the Earth and Moon* (eds. R. Canup and K. Righter), pp. 265–289. Lunar and Planetary Institute and University of Arizona Press, Tucson, Arizona, USA.

WASSON J. T. AND KALLEMEYN G. W. (1988) Composition of chondrites. *Phil. Trans. Royal Soc. Lond.* **A325**, 535–544.

WASSON J. T. AND WANG S. (1991) The histories of ordinary chondrite parent bodies: U,Th-He age distributions. *Meteoritics* **26**, 161–167.

WULF A. V., PALME H. AND JOCHUM K. P. (1995) Fractionation of volatile elements in the early solar system: Evidence from heating experiments on primitive meteorites. *Planet. Space Sci.* **43**, 451–468.

YAMAGUCHI A., SCOTT E. R. D. AND KEIL K. (1999) Origin of a unique impact-melt rock: The L-chondrite Ramsdorf. *Meteorit. Planet. Sci.* **34**, 49–59.

YOLCUBAL I., SACK R. O., WANG M-S. AND LIPSCHUTZ M. E. (1997) Formation conditions of igneous regions in ordinary chondrites: Chico, Rose City, and other heavily shocked H and L chondrites. *J. Geophys. Res.* **102**, 21 589–21 611.